Electronic Supplementary Material (ESI) for Journal of Materials Chemistry B.

Supporting Information

Fe^{3+}-coordination Mediated Synergistic Dual-network Conductive Hydrogel as Sensitive and Highly-stretchable Strain Sensor with Adjustable Mechanical Properties

Xueying Sun, Haixiao Wang, Yi Ding, Yuanqing Yao, Yaqing Liu, Jun Tang*

Department of Polymer Science, College of Chemistry, Jilin University, Changchun 130012, China

*Corresponding author.

Email: chemjtang@jlu.edu.cn.

Tel./Fax: +86-431-88498179.

Table S1 The ratio of components

AAm (g)	AA (g)	β-CD (g)	H_2O (mL)	$FeCl_3 \cdot 6H_2O$ (M)	ANI in ANI-HCl (vt%)	HCl in ANI-HCl (M)	Sample
4	1.12	1	11	0.1	3	0.12	PANI-P(AAm-*co*-AA)@Fe^{3+} (0.12 M)
4	1.12	1	11	0.1	3	0.25	PANI-P(AAm-*co*-AA)@Fe^{3+} (0.25 M)
4	1.12	1	11	0.1	3	0.39	PANI-P(AAm-*co*-AA)@Fe^{3+} (0.39 M)
4	1.12	1	11	0.1	3	0.40	PANI-P(AAm-*co*-AA)@Fe^{3+} (0.40 M)
4	1.12	1	11	0.1	3	0.41	PANI-P(AAm-*co*-AA)@Fe^{3+} (0.41 M)
4	1.12	1	11	0.1	3	0.42	PANI-P(AAm-*co*-AA)@Fe^{3+} (0.42 M)
4	1.12	1	11	0.1	3	0.43	PANI-P(AAm-*co*-AA)@Fe^{3+} (0.43 M)
4	1.12	1	11	0.1	3	0.5	PANI-P(AAm-*co*-AA)@Fe^{3+} (0.5 M)
4	1.12	1	11	0.1	3	1.0	PANI-P(AAm-*co*-AA)@Fe^{3+} (1.0 M)
4	1.12	1	11	0.1	3	1.5	PANI-P(AAm-*co*-AA)@Fe^{3+} (1.5 M)
4	1.12	1	11	0.1	3	2.0	PANI-P(AAm-*co*-AA)@Fe^{3+} (2.0 M)

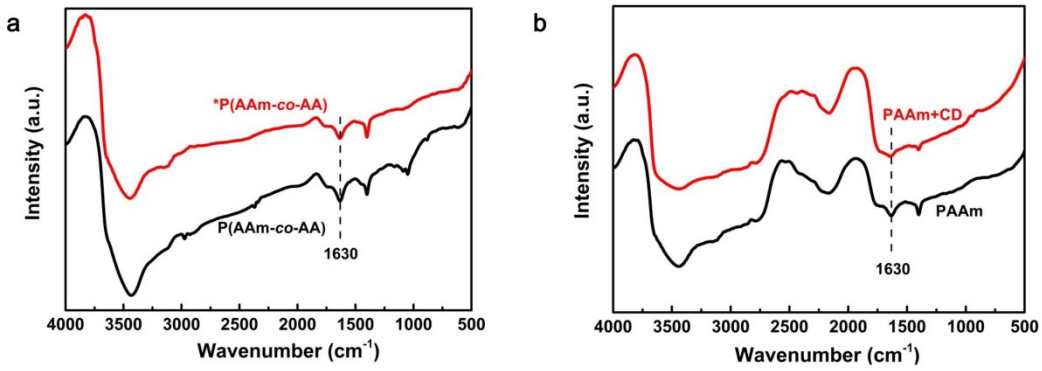

Fig. S1 FTIR spectra of (a) P(AAm-*co*-AA) and *P(AAm-*co*-AA), (b) PAAm and PAAm+β-CD.

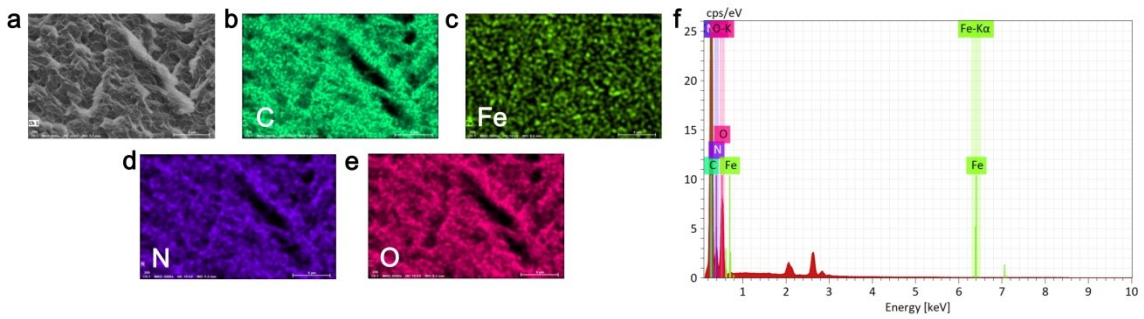

Fig. S2 (a-e) SEM images of PANI-P(AAm-*co*-AA)@Fe^{3+} with corresponding EDX elemental mapping images of C, Fe, O, N; (f) EDX spectrum of PANI-P(AAm-*co*-AA)@Fe^{3+}.

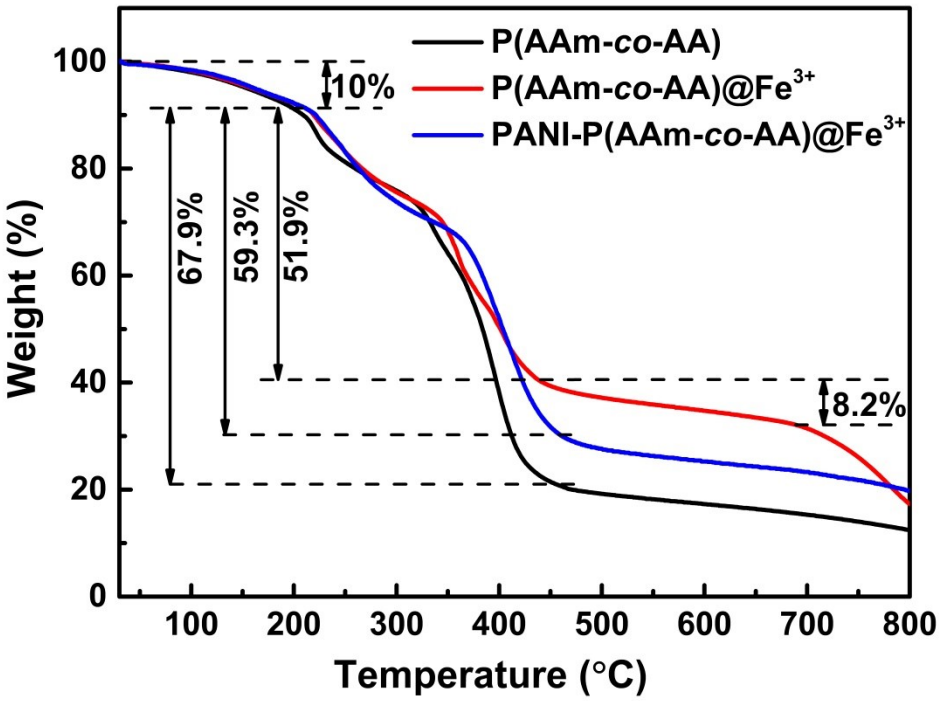

Fig. S3. TGA curves of P(AAm-*co*-AA), P(AAm-*co*-AA)@Fe^{3+} and PANI-P(AAm-*co*-AA)@Fe^{3+}.

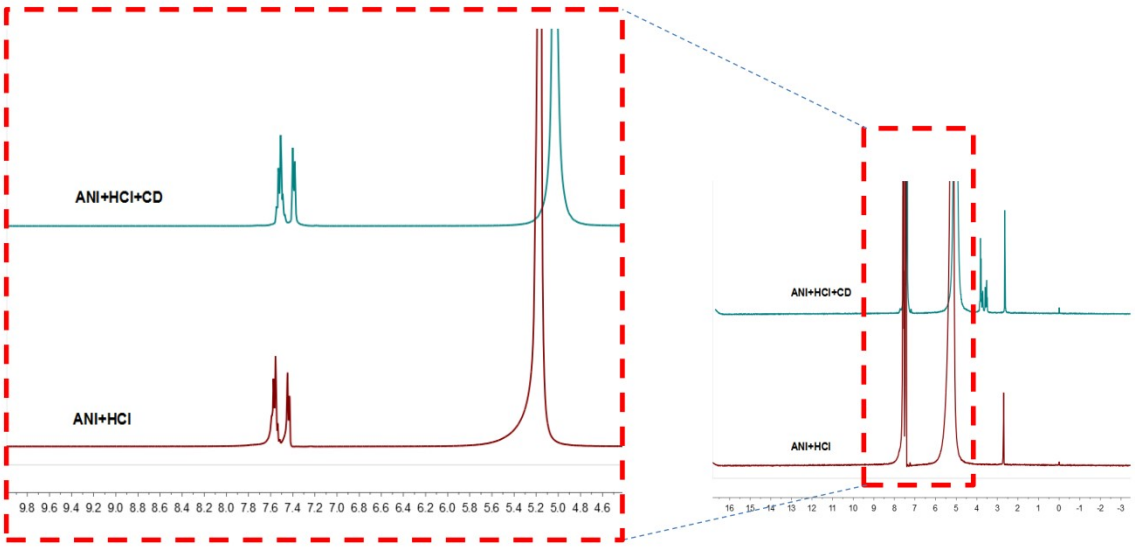

Fig. S4 ^{1}H-NMR spectra of ANI and ANI+β-CD in HCl solution in D_2O-DMSO (v/v=5:1) with tetramethylsilane (TMS) as the internal standard.

Table S2 Phenomenon of PANI-P(AAm-*co*-AA)@Fe^{3+} and solution when prepared at different acidity for 24 h.

	2 M	1.5 M	1.0 M	0.5 M	0.25 M	0.12 M
Hydrogel	Dark green and the gel becomes a viscous fluid rapidly	Dark green and the gel becomes a viscous fluid after 10 min	Dark green and the gel becomes a viscous fluid after 2 h	Dark green and the gel becomes a viscous fluid after 20 h	Dark green substance attached to the surface	Unchanged
Solution	-	-	-	-	Faint yellow	Unchanged

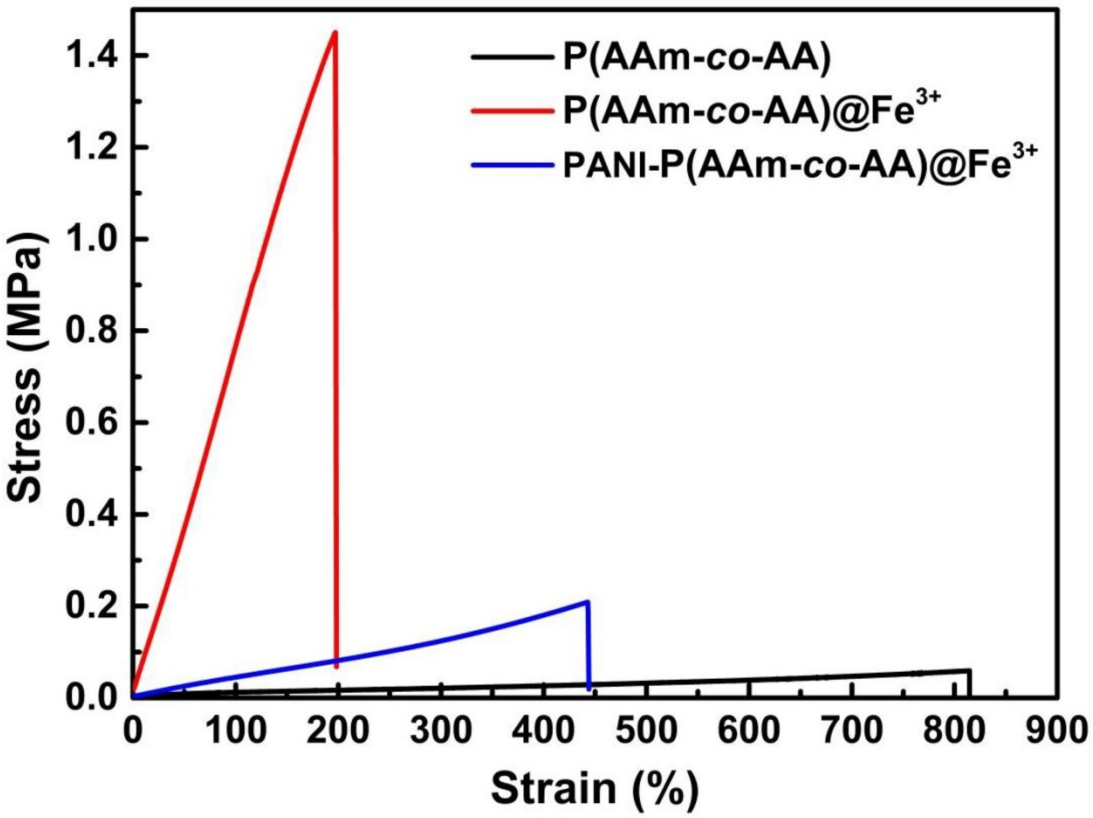

Fig. S5 Tensile strain curves of P(AAm-*co*-AA), P(AAm-*co*-AA)@Fe^{3+} and PANI-P(AAm-*co*-AA)@Fe^{3+}.

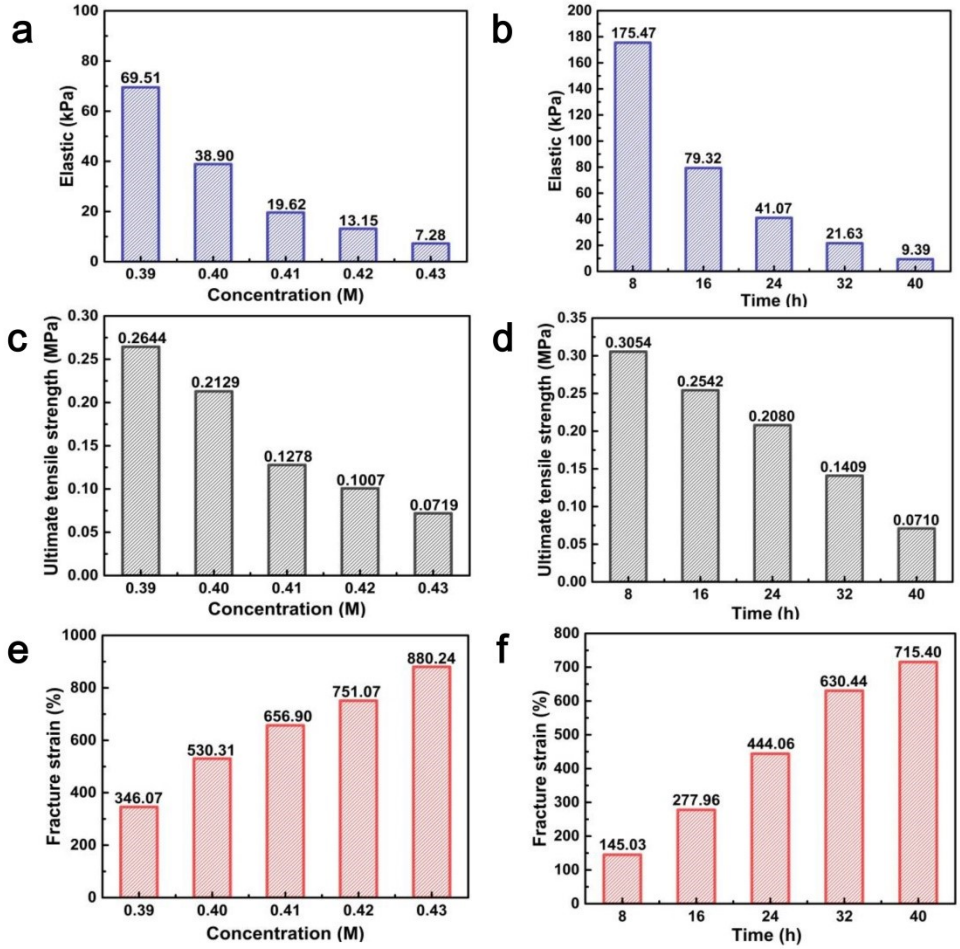

Fig. S6 The elastic, ultimate tensile strength and fracture strain of (a, c, e) PANI-P(AAm-*co*-AA)@Fe^{3+} prepared by oxidation in 3% ANI-HCl solution with different acidity for 24 h and (b, d, f) PANI-P(AAm-*co*-AA)@Fe^{3+} prepared in 3% ANI-HCl solution with the acidity of 0.40 M for different oxidation time.

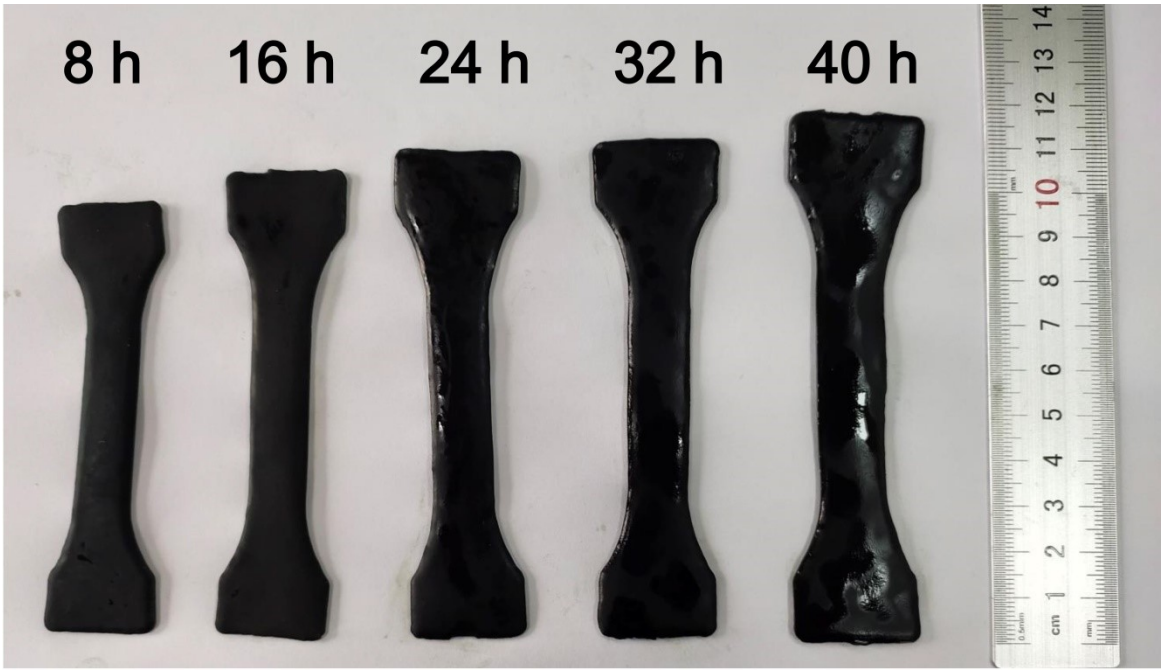

Fig. S7 Changes in the appearance of PANI-P(AAm-*co*-AA)@Fe^{3+} with different oxidation time.

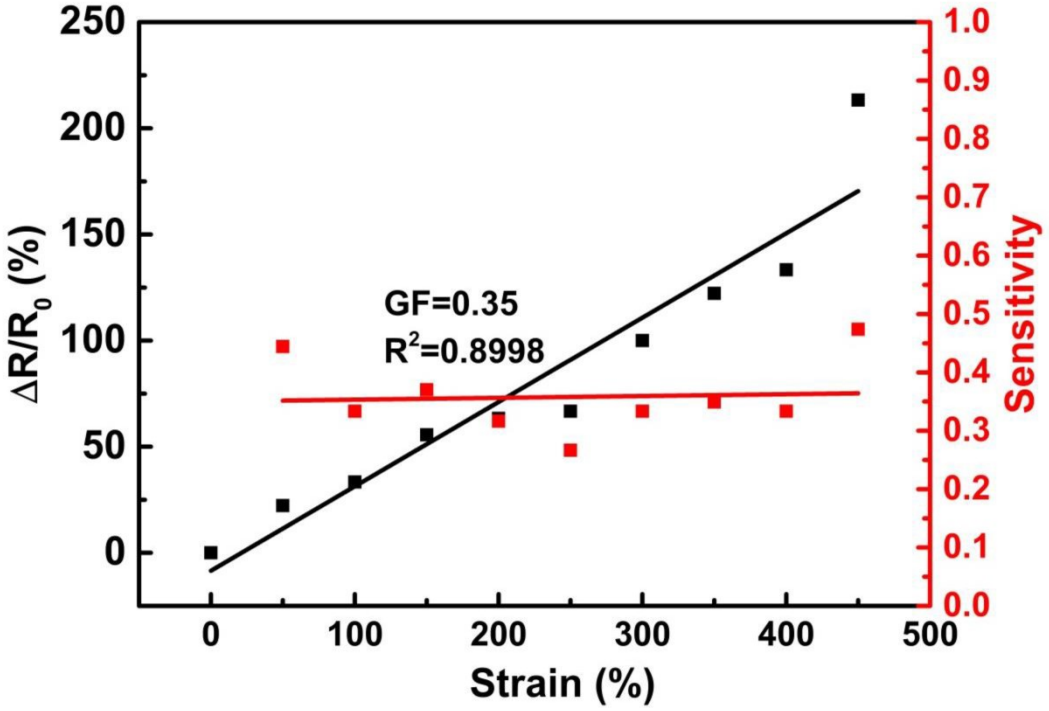

Fig. S8 Relative resistance change ($\Delta R/R_0$) and sensitivity of PANI-P(AAm-*co*-AA)@Fe^{3+} (prepared in 3% ANI-HCl solution with the acidity of 0.39 M for 24 h) under strain.

Table S3 Comparison of the performances of PANI-P(AAm-*co*-AA)@Fe^{3+} and other PANI-based conductive hydrogel materials.

Materials	Sensing range	Stress	Gauge factor	Reference
PAAm-PANI hydrogel	<300%	0.6 MPa	5.7 (low strain) 1.48 (40%-300%)	[1]
PAAm-CSM-PANI hydrogel	<85% (Compression)	6 MPa	0.35 (<1 kPa) 0.05 (1-10 kPa) 10^{-5} (>500 kPa)	[2]
PANI-PSS hydrogel	<300%	4 kPa	0.034	[3]
PANI-PAA-Phytic acid hydrogel	<400%	1.6 MPa	0.116 (100%) 0.047 (100%-400%)	[4]
PVP/PVA/CNCs-Fe^{3+} hydrogel	<200%	0.25 MPa	0.478	[5]
APP hydrogel	<140%	2.56 MPa	0.16 (0-100%) 0.39 (100%-130%)	[6]
BSP-PANI hydrogel	<525%	0.218 MPa	0.85	[7]
PANI-P(AAm-*co*-AA)@Fe^{3+}	<715.4%	0.071-0.3054 MPa	0.45	This Work

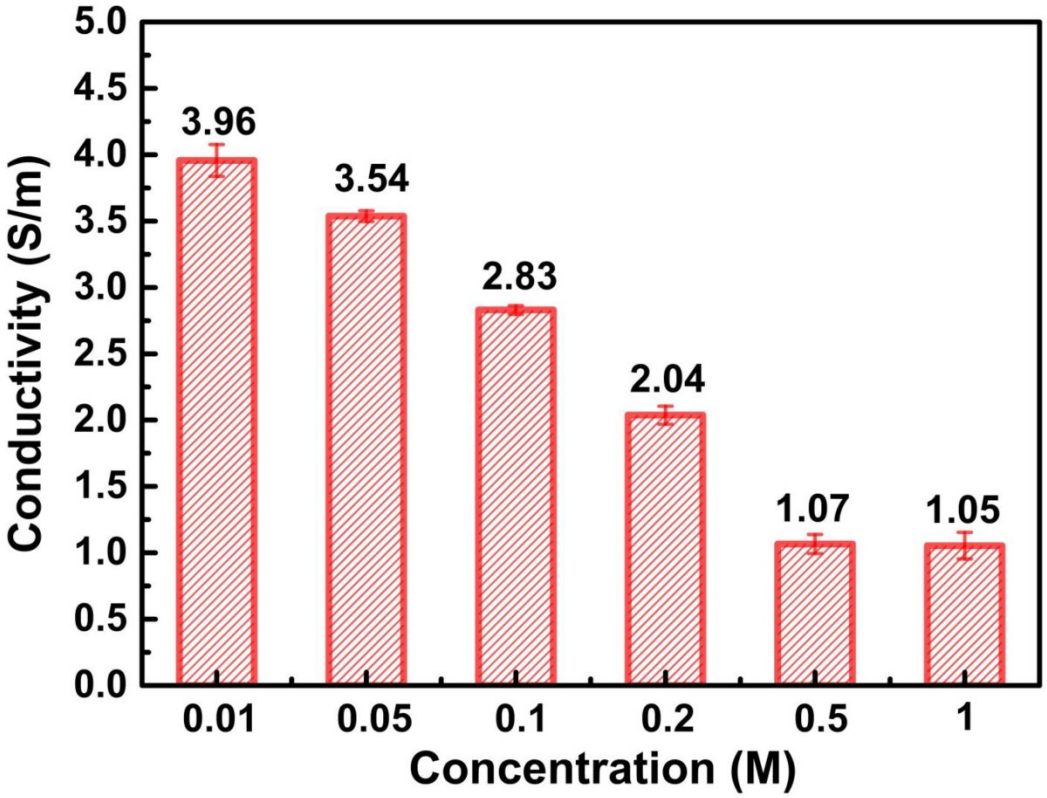

Fig. S9 Conductivity of PANI-P(AAm-*co*-AA)@Fe^{3+} prepared with different Fe^{3+} concentration.

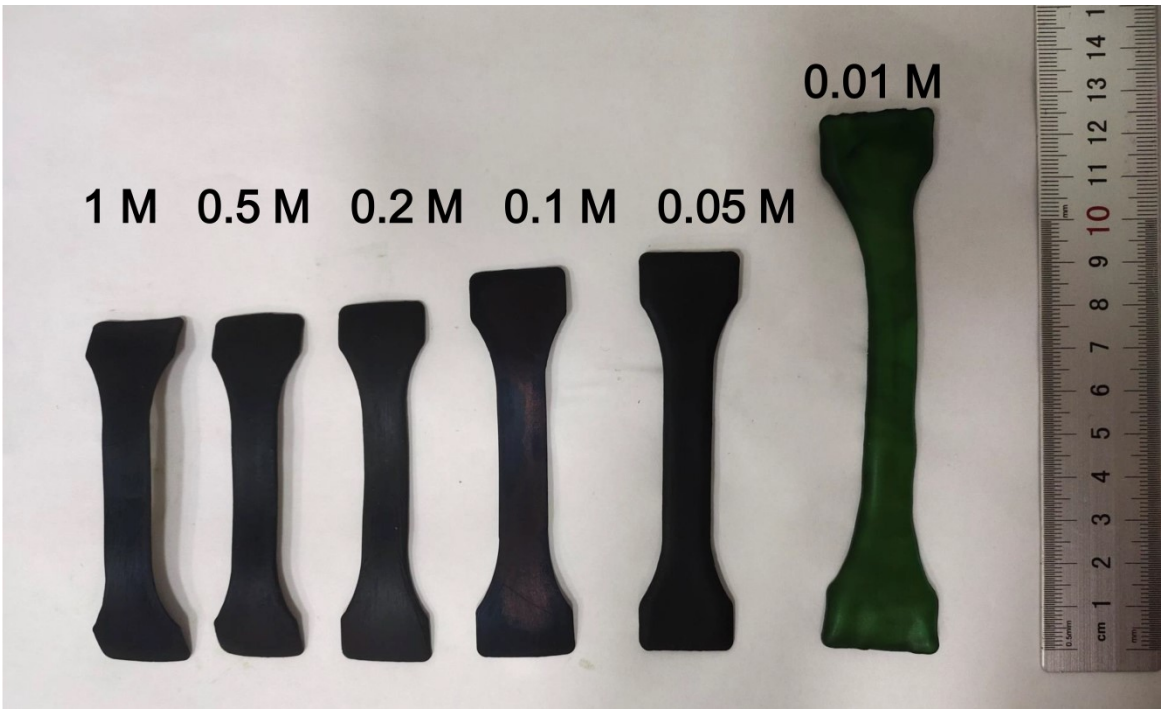

Fig. S10 Photo of PANI-P(AAm-*co*-AA)@Fe^{3+} prepared with different Fe^{3+} concentration.

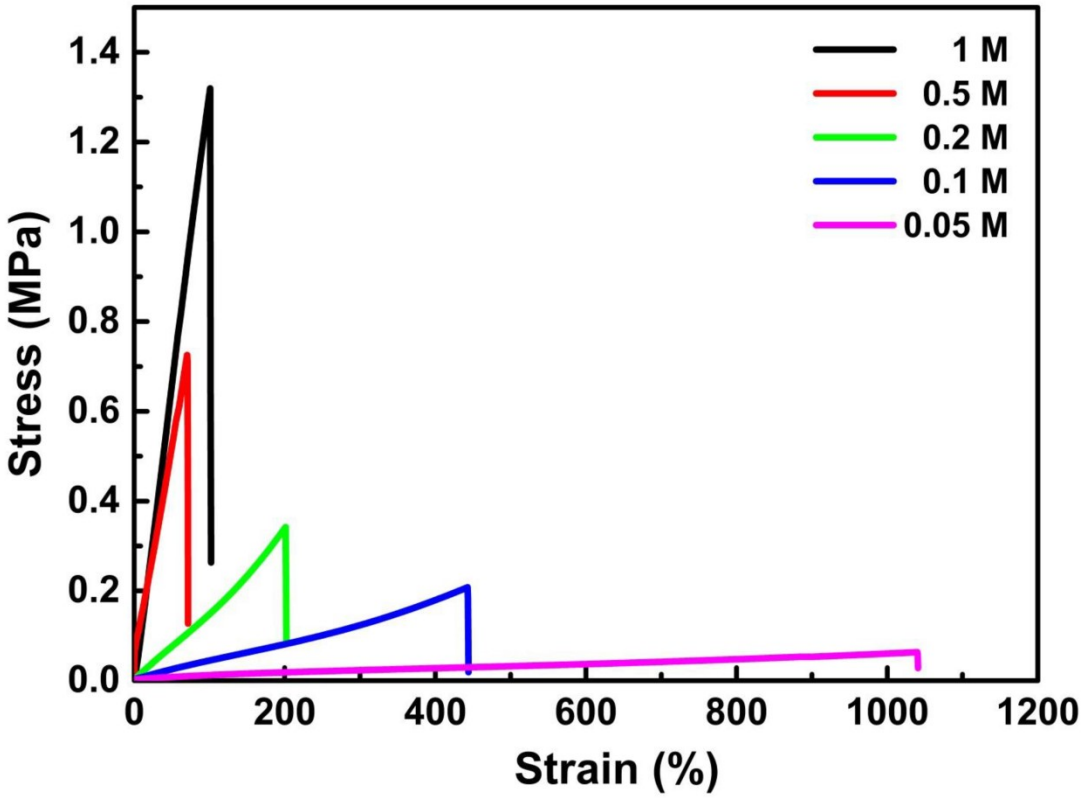

Fig. S11 Tensile curves of PANI-P(AAm-*co*-AA)@Fe^{3+} prepared with different Fe^{3+} concentration.

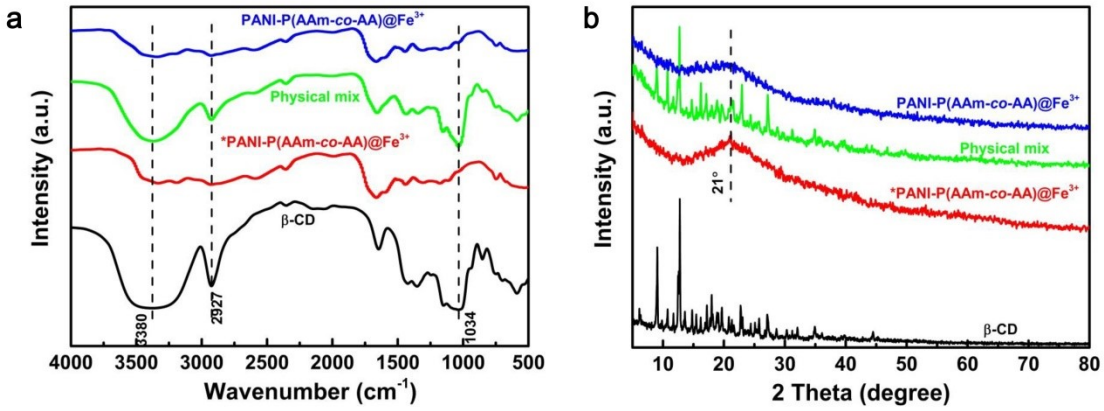

Fig. S12 (a) Infrared spectra of β-CD, *PANI-P(AAm-*co*-AA)@Fe^{3+}, physical mixture of *PANI-P(AAm-*co*-AA)@Fe^{3+} and β-CD and PANI-P(AAm-*co*-AA)@Fe^{3+}; (b) XRD patterns of β-CD, *PANI-P(AAm-*co*-AA)@Fe^{3+}, physical mixture of *PANI-P(AAm-*co*-AA)@Fe^{3+} and β-CD and PANI-P(AAm-*co*-AA)@Fe^{3+}.

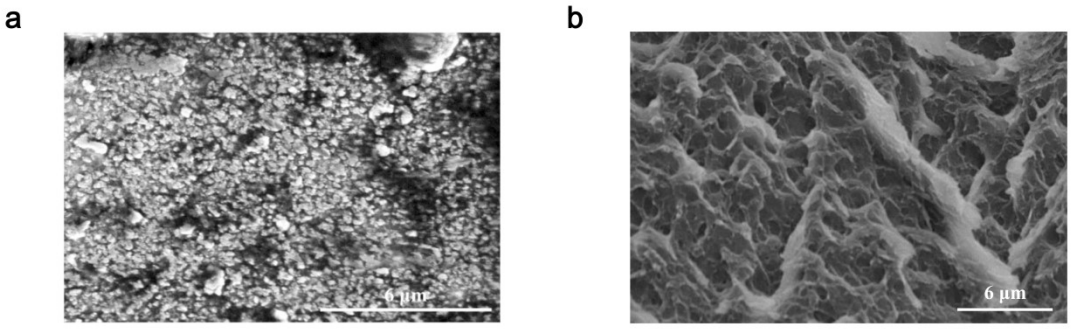

Fig. S13 SEM images of (a) *PANI-P(AAm-*co*-AA)@Fe^{3+} and (b) PANI-P(AAm-*co*-AA)@Fe^{3+}.

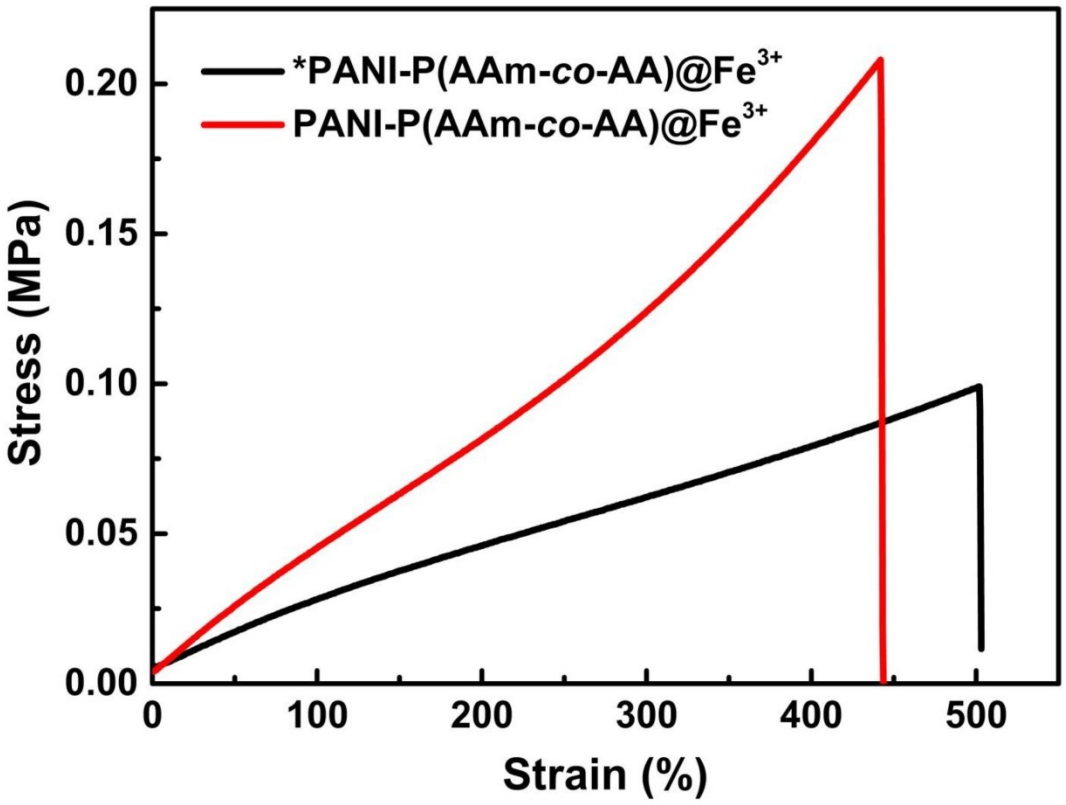

Fig. S14 Tensile curves of PANI-P(AAm-*co*-AA)@Fe^{3+} and *PANI-P(AAm-*co*-AA)@Fe^{3+}.

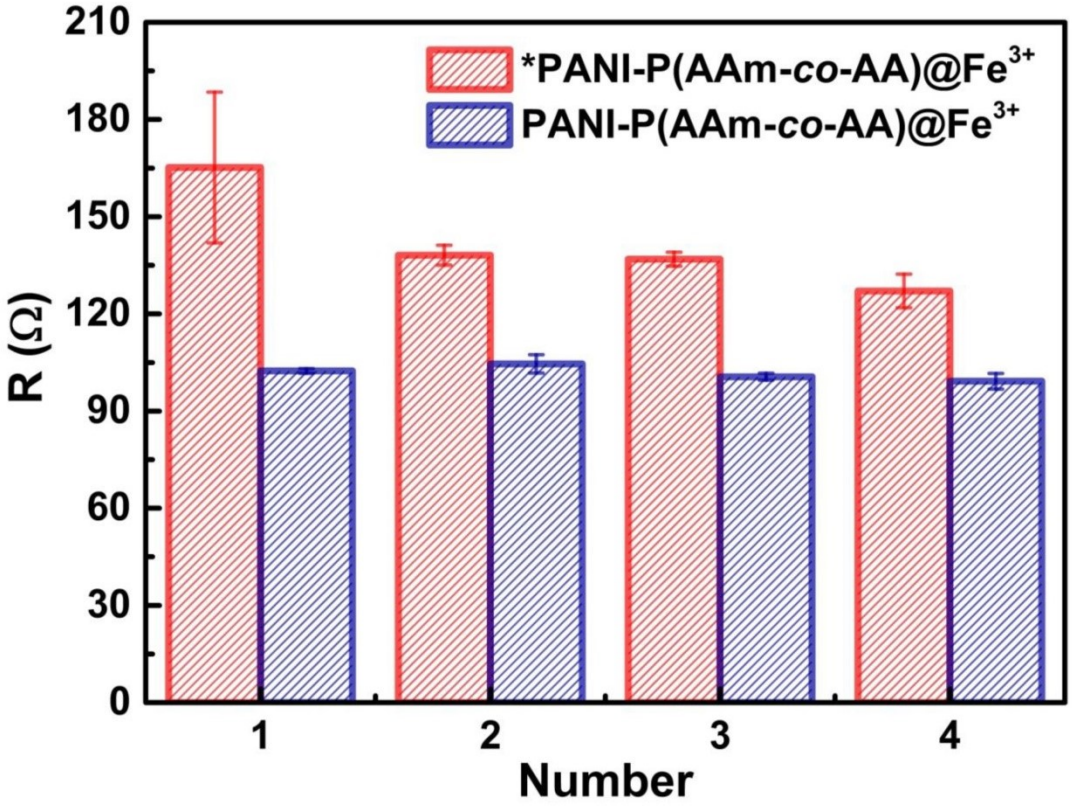

Fig. S15 Resistance and $\Delta R/\bar{R}$ of PANI-P(AAm-*co*-AA)@Fe^{3+} and *PANI-P(AAm-*co*-AA)@Fe^{3+}.

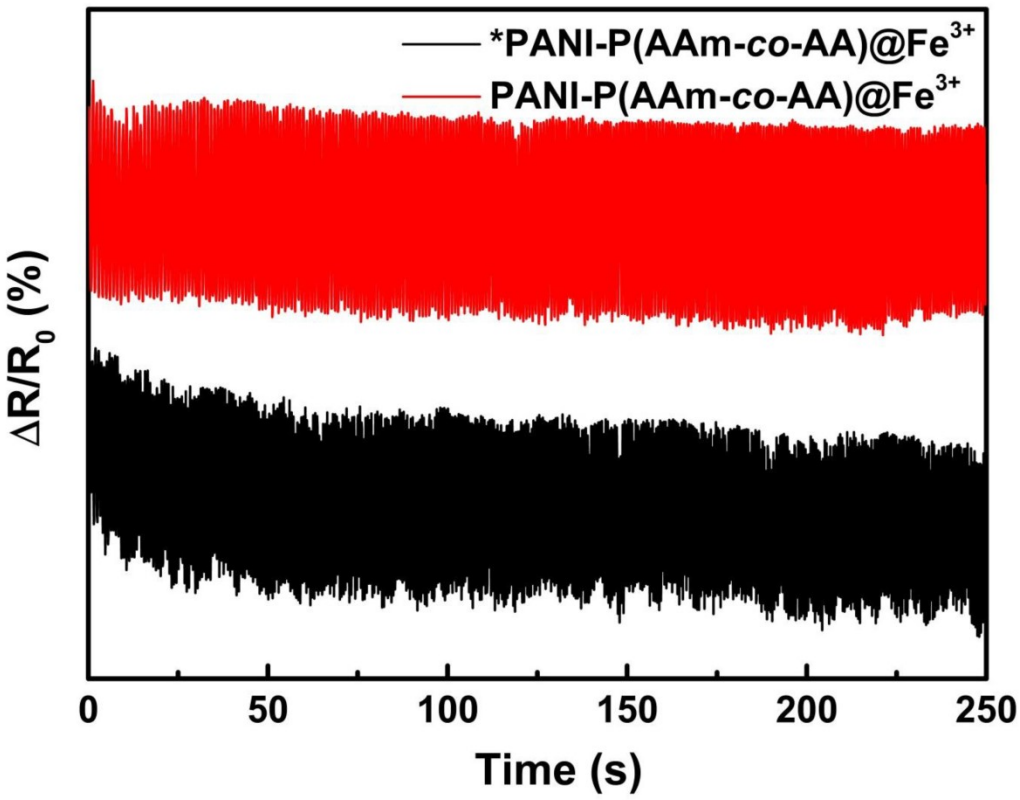

Fig. S16 Comparison of the cycle performance of PANI-P(AAm-*co*-AA)@Fe^{3+} and *PANI-P(AAm-*co*-AA)@Fe^{3+}.

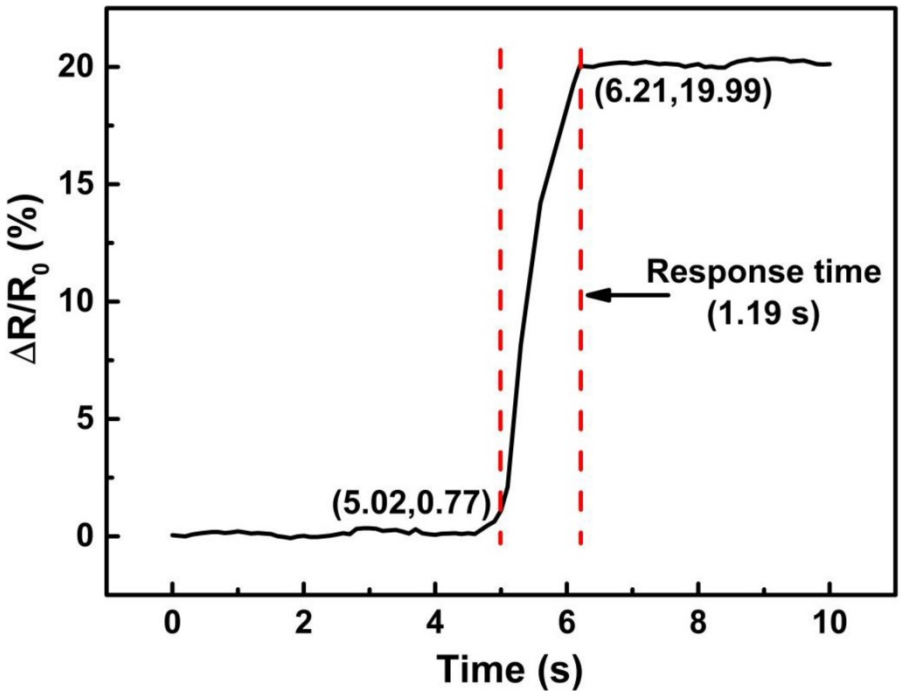

Fig. S17 Response time of PANI-P(AAm-*co*-AA)@Fe^{3+}.

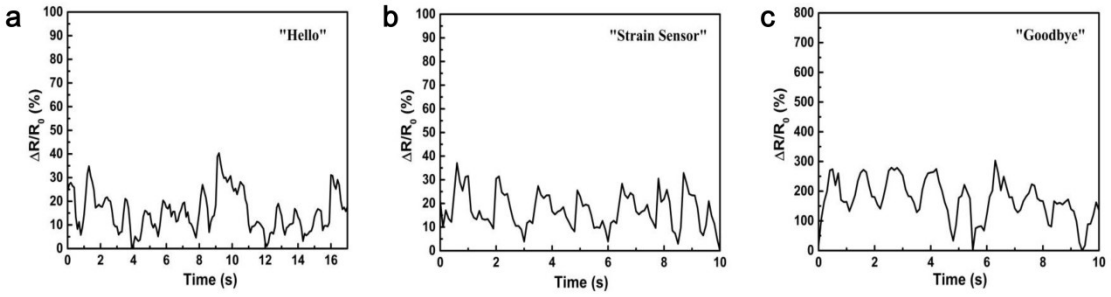

Fig. S18 $\Delta R/R_0$ signal changes of the volunteer speaking (a) “Hello”; (b) “Strain sensor” and “Goodbye”.

Notes and references

1. Z. Wang, J. Chen, Y. Cong, H. Zhang, T. Xu, L. Nie and J. Fu, *Chemistry of Materials*, 2018, **30**, 8062-8069.
2. J. Duan, X. Liang, J. Guo, K. Zhu and L. Zhang, *Adv Mater*, 2016, **28**, 8037-8044.
3. J. Chen, Q. Peng, T. Thundat and H. Zeng, *Chemistry of Materials*, 2019, **31**, 4553-4563.
4. T. Wang, Y. Zhang, Q. Liu, W. Cheng, X. Wang, L. Pan, B. Xu and H. Xu, *Advanced Functional Materials*, 2018, **28**.
5. Y. J. Liu, W. T. Cao, M. G. Ma and P. Wan, *ACS Appl Mater Interfaces*, 2017, **9**, 25559-25570.
6. J. Wang, Y. Lin, A. Mohamed, Q. Ji and H. Jia, *Journal of Materials Chemistry C*, 2021, **9**, 575-583.
7. H. Qin, Y. Chen, J. Huang and Q. Wei, *Macromolecular Materials and Engineering*, 2021, **306**.